

# We are IntechOpen, the world's leading publisher of Open Access books Built by scientists, for scientists

4,800

Open access books available

122,000

International authors and editors

135M

Downloads

Our authors are among the

154

Countries delivered to

TOP 1%

most cited scientists

12.2%

Contributors from top 500 universities



WEB OF SCIENCE™

Selection of our books indexed in the Book Citation Index  
in Web of Science™ Core Collection (BKCI)

Interested in publishing with us?  
Contact [book.department@intechopen.com](mailto:book.department@intechopen.com)

Numbers displayed above are based on latest data collected.  
For more information visit [www.intechopen.com](http://www.intechopen.com)



# Voltage-Doubler RF-to-DC Rectifiers for Ambient RF Energy Harvesting and Wireless Power Transfer Systems

*Abdul Quddious, Marco A. Antoniadou, Photos Vryonides and Symeon Nikolaou*

## Abstract

Wireless Power Transfer (WPT) is promoted as a key enabling technology (KET) for the widespread use of batteryless Internet of Things (IoT) devices and for 5G wireless networks. RF-to-DC rectifiers are essential components for the exploitation of either ambient RF power or wireless transmitted power from a dedicated source. There are several alternative rectifier topologies which can be selected depending on the desired wireless charging scenario and may include one or more diodes. For full rectification, a minimum of two diodes are needed. The current chapter discusses various implementations of voltage-doubler designs, which revolve around the basic topology of two diodes and two capacitors. Schottky diodes are usually used, in combination with lumped capacitors. Off-the-shelf diodes include both separate diodes and integrated voltage-doubler topologies in a single package. Rectifiers are inherently narrowband, non-linear devices, and the RF-to-DC efficiency, which is usually the figure of merit, depends non-linearly on both the termination load and the received RF power. The bandwidth of the rectifier depends on the preceding matching network.

**Keywords:** wireless power transfer (WPT), voltage-doubler rectifier, rectenna, RF energy harvesting and DC-to-DC booster

## 1. Introduction

In the past few decades, substantial research efforts have been devoted to wireless power transfer (WPT) applications from both dedicated [1] and ambient RF sources [2, 3]. The sensitivity of the receiver and the energy transfer efficiency are the main concerns in any WPT system, and they eventually dictate the RF energy harvesting (EH) system's performance, its range, and the overall reliability. The sensitivity depends on the minimum power that is required in order to power up the semiconductor devices used [4] in the EH circuit. On the other hand, RF-to-DC efficiency depends on the receiving antenna performance, the impedance matching network between the antenna and the rectifying circuit, and the overall

power conversion efficiency of the rectifier's subsequent stage, that is, the voltage multiplier. Traditionally, the efficiency of any rectifying circuit is controlled and improved by optimizing the circuit design [5, 6]. Additionally, it can be further improved by using a high peak-to-average power ratio (PAPR) multi-sine signals that have demonstrated improved efficiency performance compared to the conventional sinusoidal signals [7, 8]. Usually, the available ambient RF power is very low and therefore the harvested power is not sufficient to support any immediate application, although, it can be utilized to directly control the external supply dynamically [9–11]. Recently, one of the key developments in wireless communication is the exploitation of the same RF signal for information and energy harvesting. This refers to the concept of simultaneous wireless information and power transfer (SWIPT) [12] systems. Finally, RF EH is widely used in RFID tags that are used for tracking and identification [13]. With the development and integration of a low cost compact, energy harvesting circuit on the RFID tag, the conventional passive tags [14–16] can be converted into “active-equivalent” tags with improved life time and increased read range through RF energy harvesting coming from designated power beacons without relying on the reader to activate the RFID oscillating circuit [17].

To convert RF to DC power, the RF energy harvesting circuits are generally implemented using semiconductor-based rectifying elements such as CMOS diodes with transistors [18] or Schottky diodes, due to their low cost and low power requirements [4]. The most common Schottky diodes include Skywork's SMS [19] and Broadcom's HSMS [20] series of surface mount devices (SMD). **Figure 1** illustrates the basic RF-to-DC rectifier topologies. The first one (**Figure 1a**) is a single diode half-wave rectifier (envelope detector) that consists of a series diode with shunt capacitor and performs half-wave rectification by passing either the negative or the positive half of the AC current while the remaining half is blocked. Single diode, half-wave rectifiers have large rectified voltage ripples compared to full-wave rectifiers, hence, additional filtering is required to remove the harmonics from the DC output. The use of Schottky diodes with lower built-in threshold voltage, such as the SMS7630, contributes toward improved RF-to-DC conversion efficiency for the lower input power signals. This happens because a fixed amount of power is consumed for biasing the diodes, which for lower power signals, it is high percentage of the original RF power. The second rectifier topology (**Figure 1b**) is the voltage doubler, or single stage voltage multiplier, that works as a full-wave rectifier and converts the incident AC signal to a constant polarity voltage at its output. Compared to the half-wave rectifier, it results in a higher average DC voltage. It consists of a one-stage clamper with a pumping capacitor at the input of a shunt diode and a series rectifying diode along a shunt capacitor at the output stage, which

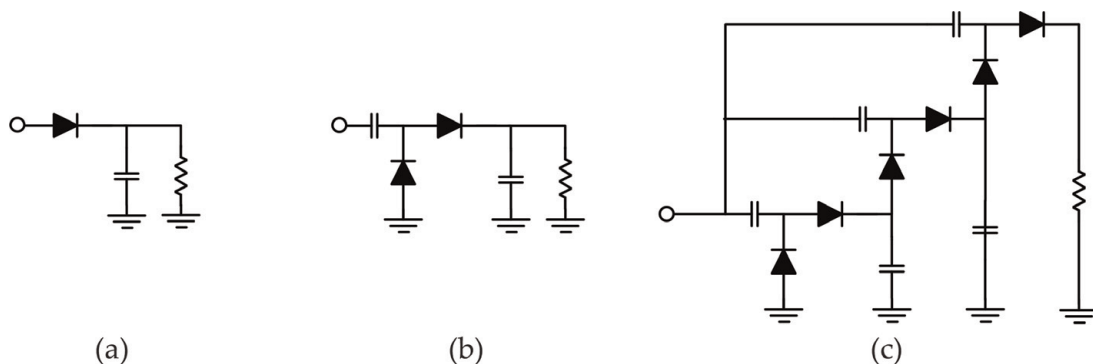


**Figure 1.** Rectifier topologies, (a) single diode (single-stage), (b) voltage doubler, and (c) voltage multiplier (multi-stage).

works as a low pass filter to smoothen the output DC voltage. The third topology (**Figure 1c**) is the voltage multiplier (multi-stage), which is a full-wave rectifier that further increases the output voltage with a network of capacitors and diodes. It has a similar operation principle to the voltage doubler. The voltage of each stage is used as a reference for the next stage, and the maximum output voltage depends on the overall number of stages. The undesired effect of the multi-stage rectifiers is the decrease in the overall efficiency which degrades for every additional stage since the efficiency of every single stage is a multiplying factor smaller than one (1). It is important to note that the overall RF-to-DC conversion efficiency depends directly on the selected topology. Where the available AC power is high, the use of multi-stage rectifiers results in an increased DC voltage level, although the overall power efficiency is decreased. For RF EH systems though, the available input power is usually very low. For relatively low input power situations where the available power is comparable to the amount of power that is required to switch on the rectifying diodes, the lower the number of diodes is, the higher the overall RF-to-DC efficiency is.

## 2. Voltage doubler

The use of the voltage doubler circuit implemented with Schottky diodes appears often in the literature. The voltage doubler circuit consists of a combination of two diodes and two capacitors connected in the topology presented in the schematic of **Figure 2a**. Several types of diodes can be used for the implementation of a voltage doubler. **Figure 2b** presents the equivalent circuit for the Skyworks SMS7630 Schottky diode, which was used for many of the rectifiers which are discussed in this chapter.

**Figure 2a** illustrates the schematic of a voltage double topology with the preceding antenna and the required matching network. The antenna and rectifier, including the intermediate matching network, are commonly referred to as a rectenna. The presented voltage doubler implementation consists of the clamper stage formed by the capacitor  $C_1$  and the diode  $D_1$ , the rectifying diode ( $D_2$ ), and the RC low pass filter ( $C_2$  and  $R_L$ ). The preceding matching network illustrated here as a box, is usually part of the rectifier circuit and it assures the maximum power transfer by reducing the impedance mismatch loss between the preceding antenna and the rectifier circuit. Often, the matching network is built with reactive lumped or distributed components, optimized for the intended operation frequency and

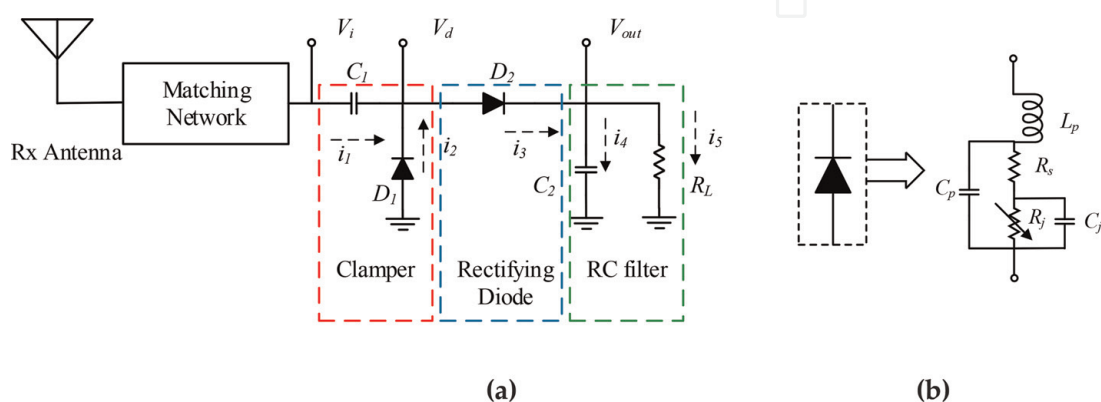


**Figure 2.** RF energy harvesting systems (a) voltage doubler circuit (b) equivalent model for Schottky diodes in voltage doubler topology.

the expected power levels, since rectifiers are non-linear devices. Several different matching topologies are discussed in the subsequent sections.

## 2.1 Voltage doubler operation principle

As the first voltage doubler stage following the matching network, the clamper is used to enhance the input voltage to the rectifying diode ( $D_2$ ), as can be seen in **Figure 2a**. Clamping circuits are mostly used to implement the voltage multiplier [8]. For a time-varying sinusoidal input signal, the clamping circuit uses the peak of the negative voltage of the input signal to produce a positive shift in the signal during its positive part, as explained below.

From **Figure 2a**,  $V_i$  is the voltage at the input of the capacitor  $C_1$ ,  $i_1$  is the current passing through  $C_1$ ,  $V_d$  is the voltage on diode  $D_1$ , and  $i_2$  is the current on  $D_1$ . The clamper is activated during the negative cycle of  $V_i$ , and  $C_1$  is charging with  $D_1$  in ON state. During the positive cycle,  $C_1$  acts as a voltage source of  $-V_{c1}$  with  $D_1$  in OFF state. According to Kirchhoff's law at the relevant loop,  $V_d$  is associated with  $V_{C1}$  and  $V_i$  through (1)

$$V_i = V_{C1} + V_d \quad (1)$$

$$i_1 = C_1 \frac{dv_{C1}}{dt} = -i_2 = -I_s \left( e^{V_d/nV_T} - 1 \right) \quad (2)$$

where  $V_d = V_{D1} \times I_s$ ,  $V_T$ ,  $I_s$ , and  $n$  show the thermal voltage, the saturation current, and the ideality factor, respectively. The voltage enhancement factor is defined as the ratio of input voltage to rectifying diode voltage  $V_d$  with peak input voltage to clamper circuit  $V_i$  [8]. For the ideal continuous wave excited voltage doubler, the voltage enhancement factor is two, if the clamper moves perfectly the input signal to the DC offset, equal to the peak of  $V_i$  during the negative input cycle.

It can be seen in **Figure 2a** that the rectifying circuit consists of the diode  $D_2$  and the low pass RC filter with capacitor  $C_2$  and termination load  $R_L$ .  $V_d$  is the input voltage and  $i_3$  is current through the diode  $D_2$ , while the current through the capacitor  $C_2$  and load resistor  $R_L$  is denoted by  $i_4$  and  $i_5$ , respectively, and the output voltage is  $V_{out}$ . According to Kirchhoff's law, the voltage across diode  $D_2$  is:

$$V_{D2} = V_d - V_{out} \quad (3)$$

where

$$i_3 = i_4 + i_5 \quad (4)$$

$$i_3 = I_s \left( e^{V_d/nV_T} - 1 \right) \quad (5)$$

$$i_4 = C_2 \frac{dV_{out}}{dt}, i_5 = V_{out}/R_L \quad (6)$$

The ordinary differential equation (ODE) by proper transformation of nonlinear behavior of the diode described in Eqs. (5) and (6) is:

$$\frac{dV_{out}}{dt} = i_5/C_2 = I_s \left( e^{V_d - V_{out}/nV_T} - 1 \right) - V_{out}/R_L C_2 \quad (7)$$

Equation (7) is a nonlinear form of an ODE, and a closed form solution for the general case is not available. Though, its numerical solution is possible using the ODE solver [8], the calculated DC output voltage is

$$V_{DC} = \frac{1}{T-t} \int_t^T V_{out}(t) dt \quad (8)$$

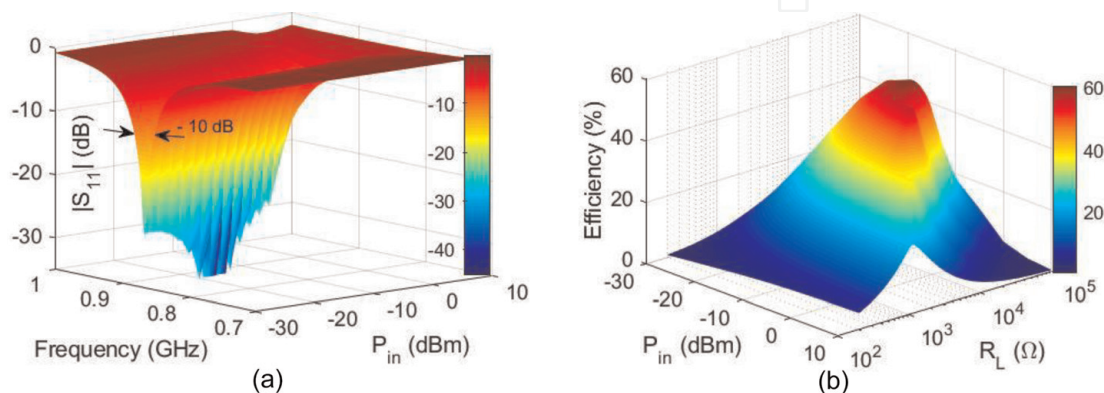
where  $t$  is the steady state charging starting time, and  $T = n\tau$  is the total number of  $n$  periods of the output signal [8].

The non-linear response of the diode is represented by a varying ohmic load  $R_j$  (see **Figure 2b**). A real diode requires a combination of parasitic capacitors and inductors, which are needed to accurately model the package of the semiconductor device. The non-linear nature of the Schottky diodes used is reflected in the matching of the rectifier device ( $|S_{11}|$ ) and also on the resulting RF-to-DC efficiency. **Figure 3a** presents the simulated reflection coefficient for a single-port voltage doubler rectifier. The reflection coefficient resonance shifts when the input power is varied and therefore a wideband matching network is needed in order to maintain the  $|S_{11}|$  below  $-10$  dB, despite the shift of the resonance. The achieved RF-to-DC efficiency also depends non-linearly on the termination load and the input RF power, as can be seen in the simulated efficiency surface presented in **Figure 3b**.



## 2.2 Implemented rectifier circuits

A thorough study of voltage-doubler rectifiers in the UHF frequency range is presented in this section, considering possible variations on (a) the diode model (b) the substrate type, and (c) several alternative matching configurations. In particular, the Broadcom HSMS2850 and the Skyworks SMS7630 Schottky diodes were investigated. The use of low-cost, lossy FR4 substrate ( $\epsilon_r = 4.3$ ,  $\tan\delta = 0.016$ ) was compared with the higher-cost and less lossy Duroid 5880 substrate ( $\epsilon_r = 2.2$ ,  $\tan\delta = 0.0009$ ). Finally, a wide range of matching circuits that consisted of one or more lumped inductors, one or more radial and custom shaped open and shorted stubs, and the use of tapered microstrip lines for bandwidth enhancement were considered in an attempt to enhance the bandwidth and the bandwidth stability for various power levels of the UHF rectifiers investigated.

For this study, 11 rectifier variations were fabricated and measured. The fabricated rectifiers labeled A to K with a short description of their characteristics, matching networks, and diodes used are presented in **Table 1**. The first comparison between a voltage-doubler rectifier (Rectifier A) and a single-stage rectifier (Rectifier B) presented in **Figure 4** suggests that for input power levels higher than  $-15$  dBm, the voltage doubler topology exhibits a higher RF-to-DC efficiency. For most wireless power transfer applications and due to the unavoidable free-space



**Figure 3.** Non-linearity of the rectifying circuit (a) simulated  $|S_{11}|$  versus frequency and input power (b) efficiency percentage vs. input power and termination load.

Rect.	Schematic	Description (matching network)	Diode
A		Consists of low-loss distributed elements, which include shorted stub, two-stage tapered line, radial stub followed by distributed inductor	SMS7630
B		Consists of low-loss distributed elements, which include shorted stub, two-stage tapered line, radial stub followed by distributed inductor	SMS7630
C		Consists of distributed elements, which include a shorted stub and a radial stub at the beginning and at the end of a U-shaped microstrip line	HSMS2850
D		Consists of distributed elements, which include a shorted stub and a radial stub	SMS7630
E		Consists of a hybrid matching network, which includes a radial stub, a shorted stub, and a series inductor	HSMS2850
F		Consists of a hybrid matching network, which includes a radial stub and two series inductors	SMS7630
G		Consists of low-loss distributed elements, which include a shorted stub, a radial stub followed by a distributed inductor	HSMS2850
H		Consists of low-loss distributed elements, which include a shorted stub, a radial stub followed by a distributed inductor	HSMS2850
I		Consists of low-loss distributed elements, which include a shorted stub, two-stage tapered line, a radial stub followed by a distributed inductor	SMS7630
J		Consists of a hybrid matching network, which includes a radial stub and two series inductors	SMS7630
K		Consists of a hybrid matching network, which includes a radial stub and two series inductors	HSMS2850

**Table 1.**  
Implemented rectifiers labeled A to K.

loss, the available power at the receiver is rather low. However, the received power level is random and cannot be predicted, and the efficiency plots for Rectifiers A and B cross at the  $-15$  dB input power mark (**Figure 4d**), therefore a direct comparison of the efficiency performance is not straight forward. The improved average efficiency performance over the entire power range is the main reason why the voltage doubler was preferred over the single stage rectifier and was further studied in detail. The free-space loss is inversely proportional to  $\lambda^2$  and this is the reason why the UHF frequency (relatively low frequency) was preferred for the presented study.

### 2.3 Voltage doubler matching considerations

Rectifiers C, D, E, and F were designed on an FR-4 substrate, and are used to discuss the effect of the matching circuit on the stability of the  $|S_{11}|$  resonance that defines the matching, and on the  $-10$  dB bandwidth of the  $|S_{11}|$ . As can be seen from **Figures 5** and **6**, the matching depends on the input power level. For different power levels, the exact position of the resonance that defines the matching ( $|S_{11}| < -10$  dB) shifts, and for certain values, the rectifier is mismatched, and as a result, the RF-to-DC efficiency degrades. Rectifiers C and D, which are compared in **Figure 5**, use different diode types, (Broadcom and Skyworks, respectively), and

similar matching networks that consist of shorted and radial matching stubs. The  $|S_{11}|$  resonance remains rather stable as the input power varies, but it is narrowband ( $\sim 25$  MHz). The different diode models have minimum effect on the matching, but

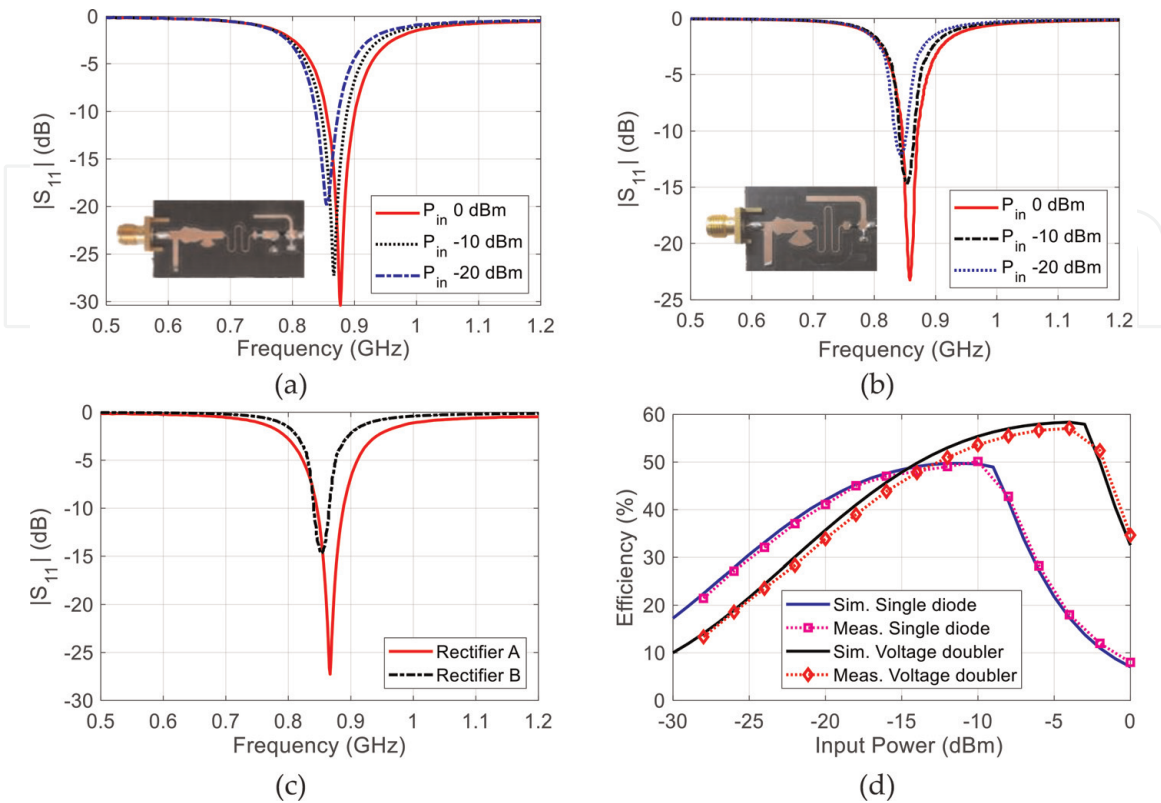


**Figure 4.** Voltage doubler (A) and single stage rectifier (B) comparison; (a) Rectifier A  $|S_{11}|$ , (b) Rectifier B  $|S_{11}|$ , (c)  $|S_{11}|$  at  $-10$  dBm comparison, and (d) RF-to-DC efficiency.

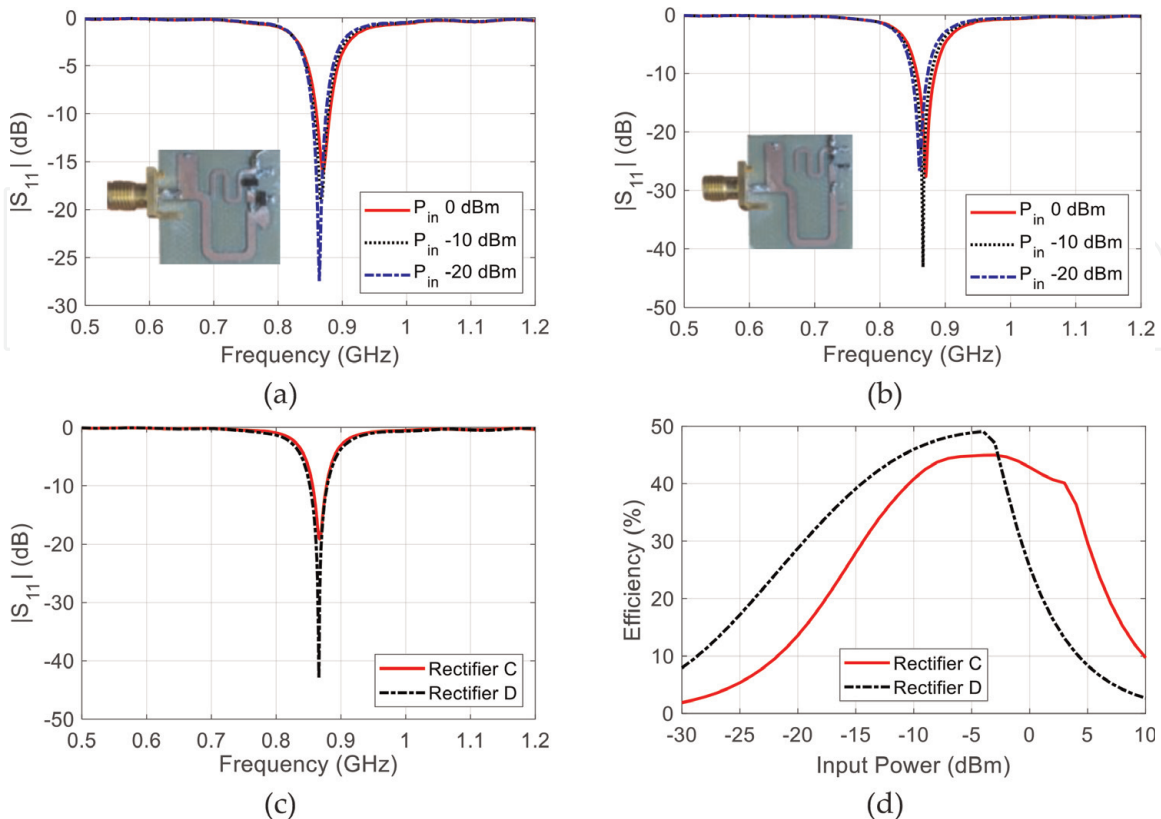


**Figure 5.** Rectifier (C) and rectifier (D) comparison; (a) Rectifier C  $|S_{11}|$ , (b) Rectifier D  $|S_{11}|$ , (c)  $|S_{11}|$  at  $-10$  dBm comparison, and (d) RF-to-DC efficiency.



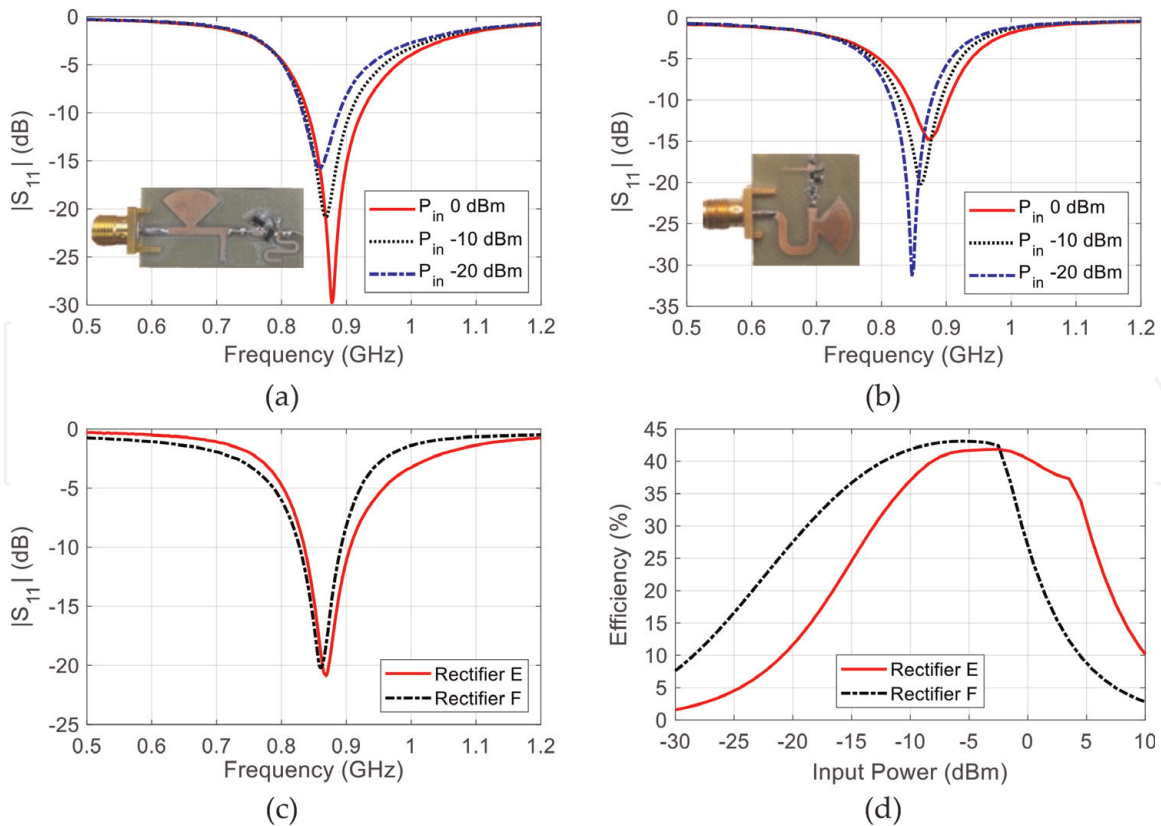


**Figure 6.**

Rectifier E and rectifier F comparison; (a) Rectifier E  $|S_{11}|$ , (b) Rectifier F  $|S_{11}|$ , (c)  $|S_{11}|$  at  $-10$  dBm comparison, and (d) efficiency.

they affect the efficiency as will be discussed subsequently. For Rectifiers E and F, presented in **Figure 6**, that use a combination of radial stubs with series inductors, the  $|S_{11}|$  shift is much more evident. For this hybrid matching circuit, what overcomes the mismatch problem in the UHF frequency is the considerably wider bandwidth (greater than 65 MHz) for both rectifiers. Apparently, the combination of radial stubs with lumped inductors and the resulting hybrid matching network enhances the bandwidth and makes the matching more tolerant to frequency shifts.

## 2.4 RF-to-DC efficiency

For any RF-to-DC rectifier, the figure of merit is the RF-to-DC efficiency, which has been shown to depend non-linearly on both the input power and the termination load, as can be verified from **Figure 3b**. In an attempt to identify the design parameters that affect the efficiency, several rectifier prototypes were fabricated and tested. Parameters such as the diode type, the use of distributed or lumped inductors for the matching network and their associated losses and quality factor, or the substrate losses of the preferred fabrication board were investigated experimentally.

The Skyworks SMS7630 [19] and Broadcom HSMS2580 [20] diodes were chosen for the high-efficiency voltage doubler topologies that were investigated at low input power, because they have been the most commonly used diodes. In the recent years, the Broadcom HSMS2852 type has been a popular diode for many RF-to-DC rectifiers used for WPT systems. For low input power levels, the higher series resistance (compared to, e.g., the Broadcom HSMS-286x family) does not seem to degrade the measured efficiency. In addition to their specifications, an important role for the selection of the diodes had to do with the availability (or not) of the diode model for the Keysight - Advanced Design System (ADS) simulator. The

Spice model of the Skyworks SMS7630 diode was characterized at 1.8 GHz, and the same model was used for the UHF rectifier simulations.

S-parameter measurements of the implemented rectifier indicated a shift in the  $|S_{11}|$  resonance. The resonance shift could be remedied with the matching network, and especially by modifying the inductance values of the inductors that were used for the matching. For the Broadcom HSMS2580 diode, an ADS library model was available and the measurements indicated that the S-parameter simulations using the ADS library model were more accurate. Similar rectifier prototypes with similar matching networks using either type of Schottky diodes (C and D or E and F) were implemented.

Considering the direct comparison between the efficiency of rectifier C (Broadcom HSMS2580) and D (Skyworks SMS7630) presented in **Figure 5d**, the general observation is that the rectifier with the Skyworks diodes has better efficiency for input power less than  $-3$  dBm, and the diode with the HSMS2580 diodes has better efficiency for input power higher than  $-3$  dBm. The same behavior is verified by inspecting **Figure 6d**, where the efficiencies of rectifiers E and F are presented. This can be explained by noting that the SMS7630 diode requires a forward bias voltage between 60 and 120 mV, and it has a breakdown voltage of 2 V, while the HSMS2850 diode has a forward bias voltage between 150 and 250 mV, and it has a breakdown voltage of 3.8 V. For the implementation of high-efficiency UHF rectifiers with lower input power levels, the Skyworks SMS7630 diodes are preferred, since improved RF-to-DC efficiency can be achieved as a result of the model's lower saturation current and lower junction capacitance.

By comparing the efficiencies for rectifiers C, D, E, and F, another important observation can be made. The use of series lumped inductors for the matching circuit seems to degrade the RF-to-DC efficiency, something verified by comparing the maximum efficiency of C (46%) with E (42%) and the efficiency of D (50%) with F (42%).

For a simulated voltage doubler circuit, a real inductor was modeled as an ideal inductor in series with an ohmic resistor to model the inductor's losses. A small variation in the ohmic resistance has a direct significant impact on the simulated efficiency, as can be verified in **Figure 7**. Based on this observation, Rectifier H was fabricated using one printed distributed inductor (meander shaped thin line in the inset of **Figure 8b**) instead of lumped inductors in the matching circuit. The comparison between Rectifier H and Rectifier K is presented in **Figure 8**. Although the matching bandwidth for the rectifier with the distributed inductor decreased, the lack of ohmic losses for the packaged lumped inductor caused a small improvement

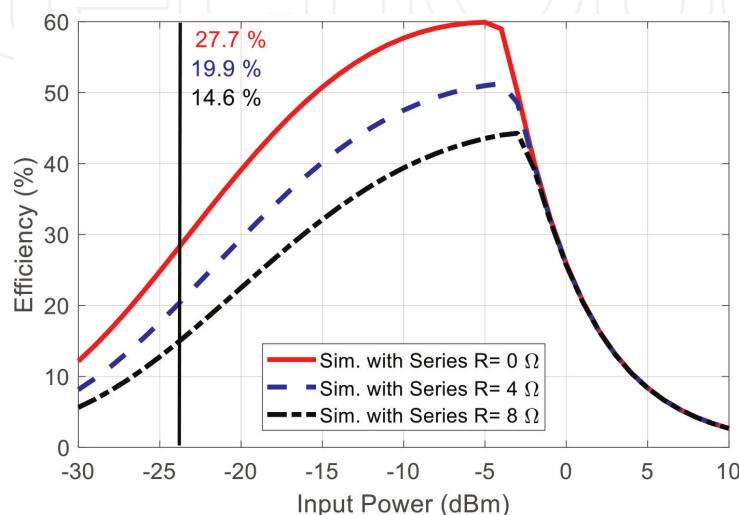


**Figure 7.**  
Effect of the ohmic losses of the lumped inductor modeled as series resistor, on the simulated efficiency.

in the efficiency, which can be verified in **Figure 8d**. This is also verified in the comparison between Rectifier A and Rectifier J presented in **Figure 9**, that were both fabricated on Rogers 5880 material. The efficiency of Rectifier A is consistently

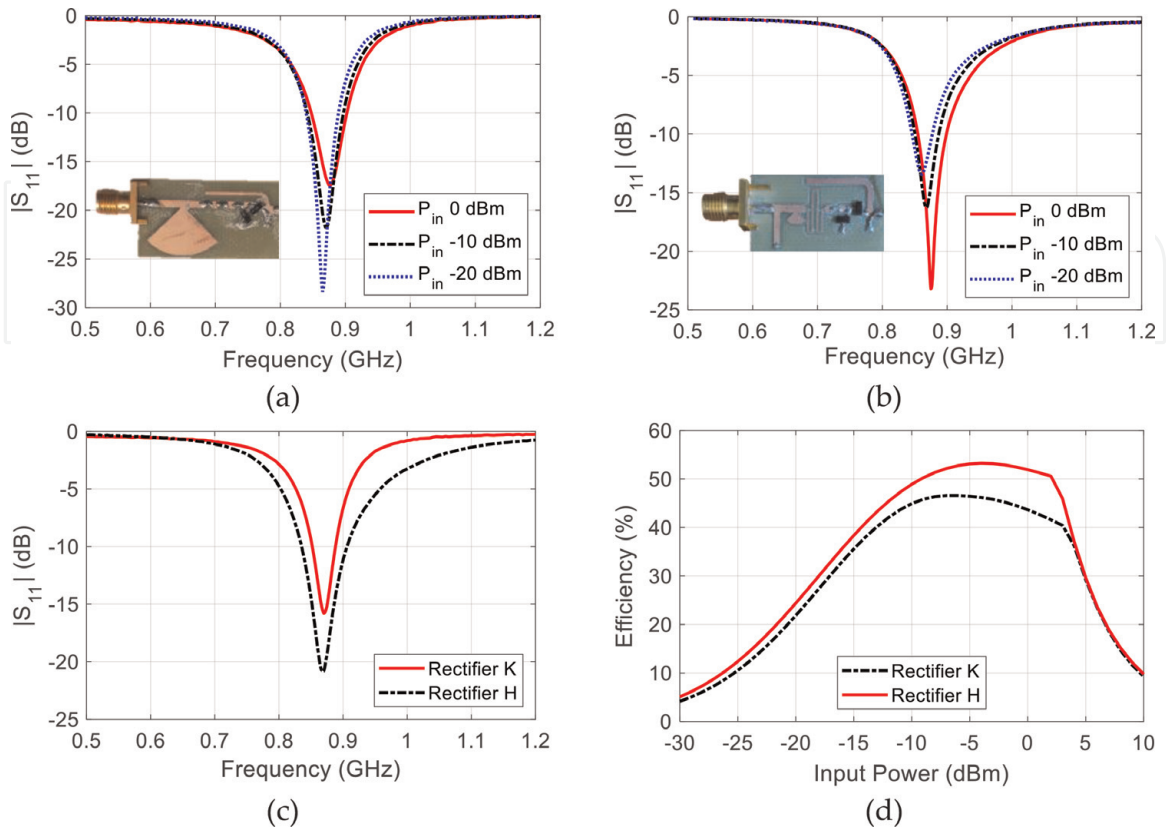


**Figure 8.** Rectifier K and rectifier H comparison; (a) Rectifier E  $|S_{11}|$ , (b) Rectifier F  $|S_{11}|$ , (c)  $|S_{11}|$  at  $-10$  dBm comparison, and (d) efficiency.

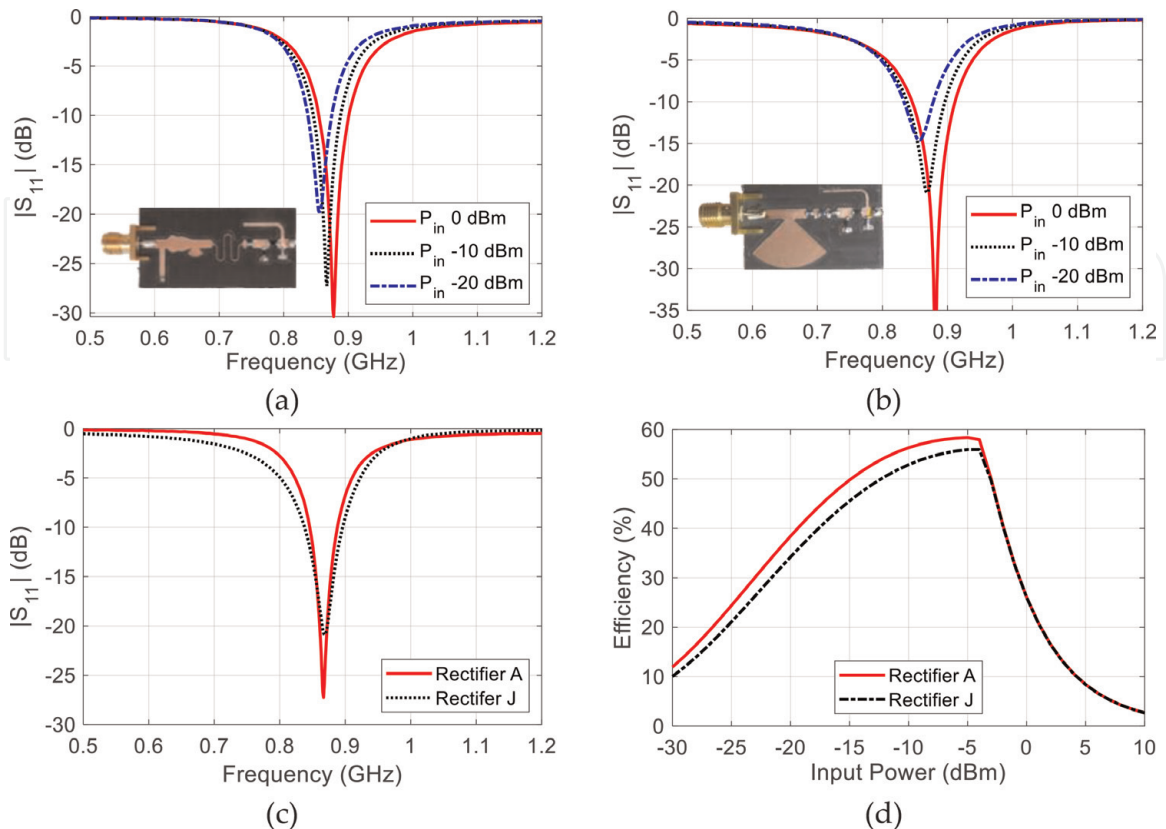


**Figure 9.** Rectifier (A) and rectifier (J) comparison; (a) Rectifier A  $|S_{11}|$ , (b) Rectifier J  $|S_{11}|$ , (c)  $|S_{11}|$  at  $-10$  dBm comparison, and (d) efficiency.

better than the efficiency of Rectifier J (**Figure 9d**), while the use of tapered lines for Rectifier A improved the bandwidth as well. Comparing the maximum efficiency of K (46%) from **Figure 8d** and the efficiency of J (56%) from **Figure 9d**, which have similar designs with the same diode models, it is obvious that the substrate losses are important in the resulting efficiency.

When distributed inductors are used instead of lumped inductors, the substrate losses become even more critical for the implemented efficiency. Low loss substrates limit the quality factor of the implemented inductors and consequently degrade the efficiency. **Figure 10a** shows the simulated rectifier efficiency when the loss tangent ( $\tan\delta$ ) of the substrate was varied. For the lower end of the input power, around  $-24$  dB, the low loss of the Rogers 5880 ( $\tan\delta = 0.009$ ) results in 30% efficiency, while for the same design,  $\tan\delta = 0.035$  reduces the efficiency to approximately 15%. For low input power, even small variations in the copper's

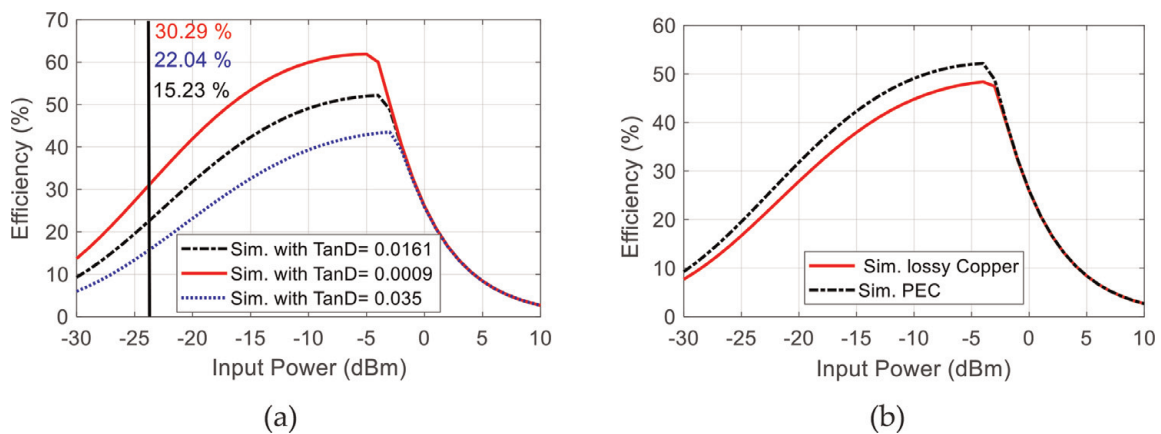


**Figure 10.** Effect of the substrate loss on the simulated efficiency (a) with variations in the loss tangent ( $\tan\delta$ ) and (b) variations in the copper's conductivity.

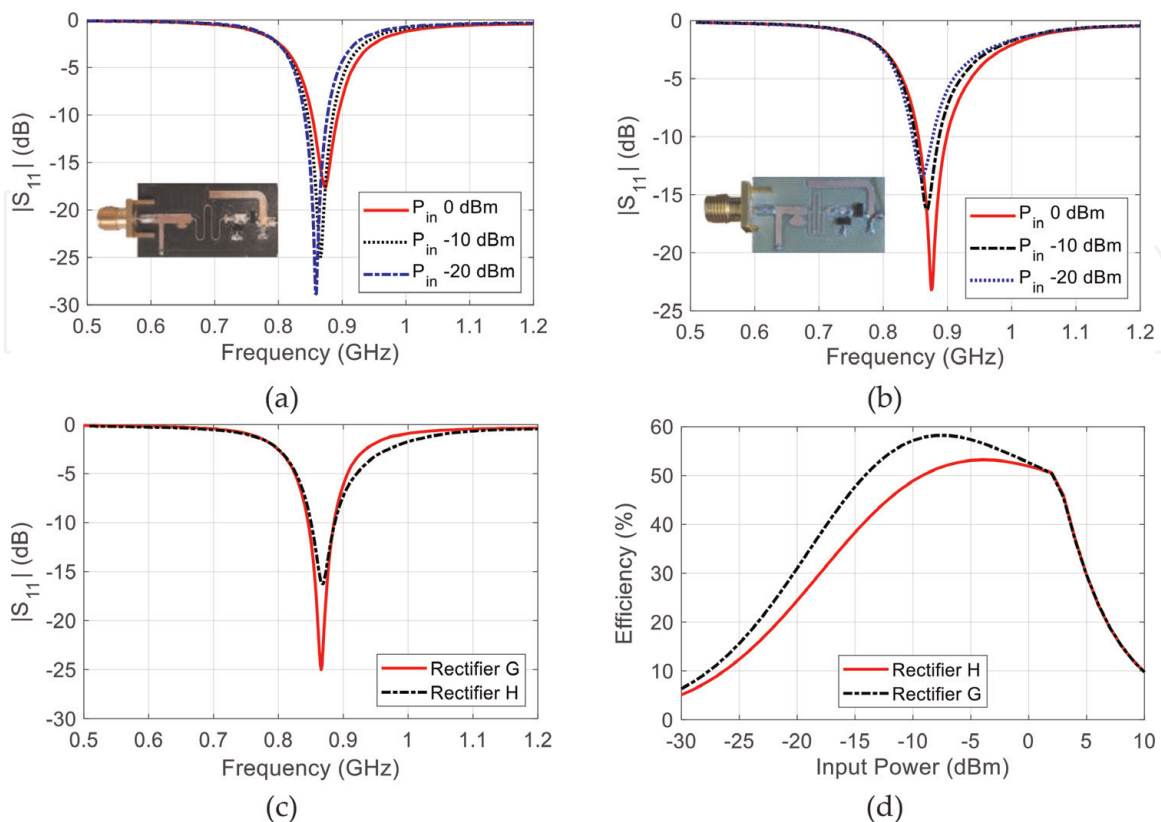


**Figure 11.** Rectifier (G) and rectifier (H) comparison; (a) Rectifier E  $|S_{11}|$ , (b) rectifier F  $|S_{11}|$ , (c)  $|S_{11}|$  at  $-10$  dBm comparison, and (d) efficiency.

conductivity affect the efficiency, as can be verified in **Figure 10b**. The importance of a low-loss substrate is evident in the measured efficiencies for the implemented rectifiers presented in **Figure 11**, where the lossy FR-4 ( $\tan\delta = 0.016$ ) was used for Rectifier H, and the more expensive low loss ( $\tan\delta = 0.0009$ ) Rogers 5880 was used for Rectifier G. **Figure 11d** verifies that the efficiency of rectifier G fabricated on the low-loss material is consistently higher than the efficiency of the similar design Rectifier H.

## 2.5 Size considerations

Considering that the fundamental voltage doubler topology that consists of two diodes and two capacitors is rather inflexible, the overall dimensions of any rectifier depend on the matching network. When a compact size is a priority, as for example in the case of implantable devices, the use of lumped components is preferred. **Figure 12** shows how the overall size of a rectifier can be significantly reduced with the use of lumped components instead of distributed ones.

Using lumped inductors for the matching network is often preferred because they can also result in a more wideband design. In order to exploit the low losses of

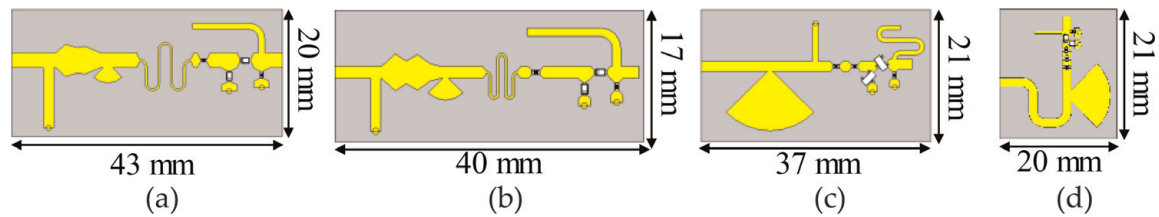


**Figure 12.** Size comparison (a) Rectifier A, (b) Rectifier I, (c) Rectifier E, and (d) Rectifier F.

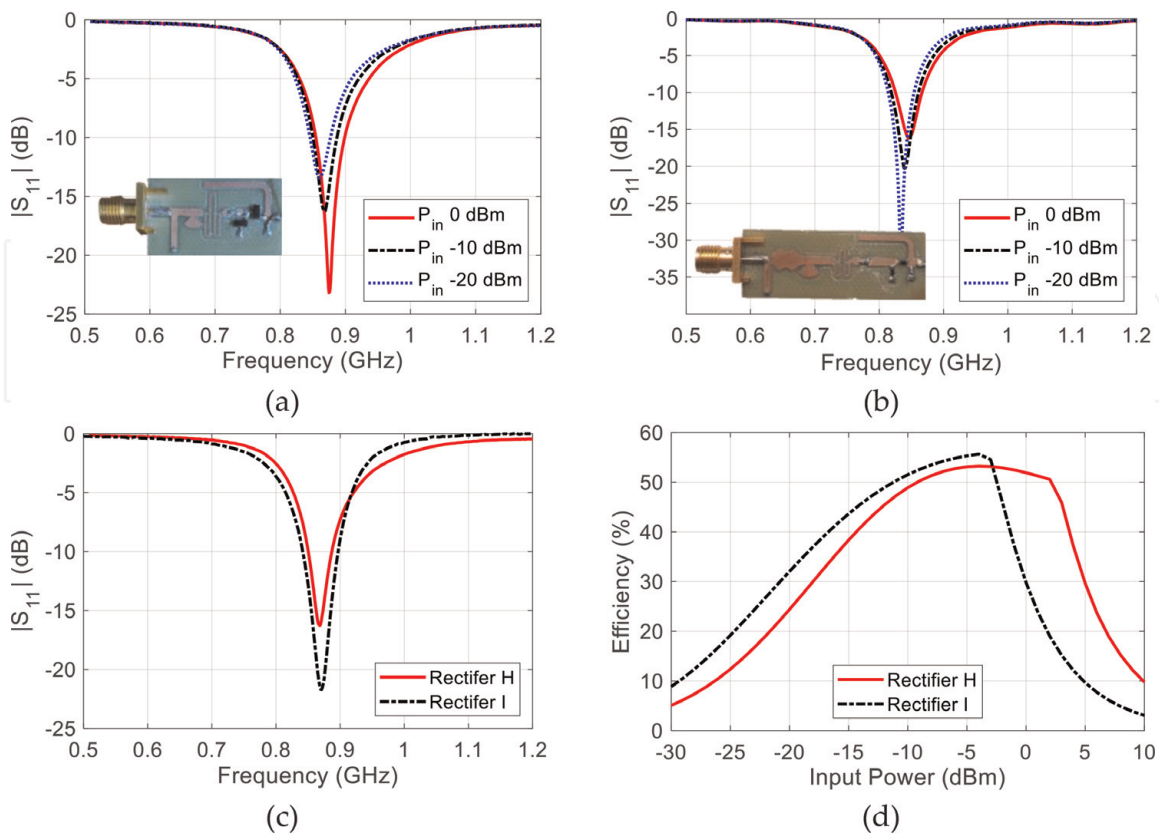


**Figure 13.** Rectifier H and Rectifier I comparison; (a) Rectifier E  $|S_{11}|$ , (b) Rectifier F  $|S_{11}|$ , (c)  $|S_{11}|$  at  $-10$  dBm comparison, and (d) efficiency.

distributed printed inductors and further improve the bandwidth of rectifiers with distributed inductors, the use of multi-stage tapered microstrip lines was considered. Rectifier I was implemented on FR-4 and used a two-stage tapered microstrip line. The performance of Rectifier I is compared with the performance of Rectifier H, which uses conventional microstrip lines, in **Figure 13**. The bandwidth of Rectifier I is 40 MHz and the bandwidth of H is 36 MHz. The 10% bandwidth enhancement (**Figure 13c**) in addition to the improved efficiency, as can be seen in **Figure 13d**, implies that if there are not strict size constraints, the best efficiency rectifier should have the following characteristics: (a) should use Skyworks 7630 diodes, (b) should use tapered microstrip lines with distributed inductors for the matching circuit, and (c) should be fabricated on low-loss material. From the implemented rectifiers A to K, Rectifier A has the aforementioned characteristics.

## 2.6 Proposed UHF rectifier – Rectifier A

The detailed design parameters of the implemented Rectifier A are presented in **Figure 14a** and are summarized in the figure caption. The matching network consists of a shorted linear stub, a two-stage tapered microstrip line for bandwidth enhancement, and a printed inductor. The maximum measured efficiency is almost 60% at  $-3$  dB. For input power higher than  $-3$  dB, the voltage saturates close to 2 V and as a result the RF-to-DC efficiency degrades, since only the denominator RF power increases while the DC power remains saturated. The simulated results presented in **Figure 14b** indicate the non-linear dependence of the efficiency with the termination load. Although the peak efficiency per power level is shifted, the rectifier parameters were optimized for a termination load equal to 13.5 k $\Omega$ . The

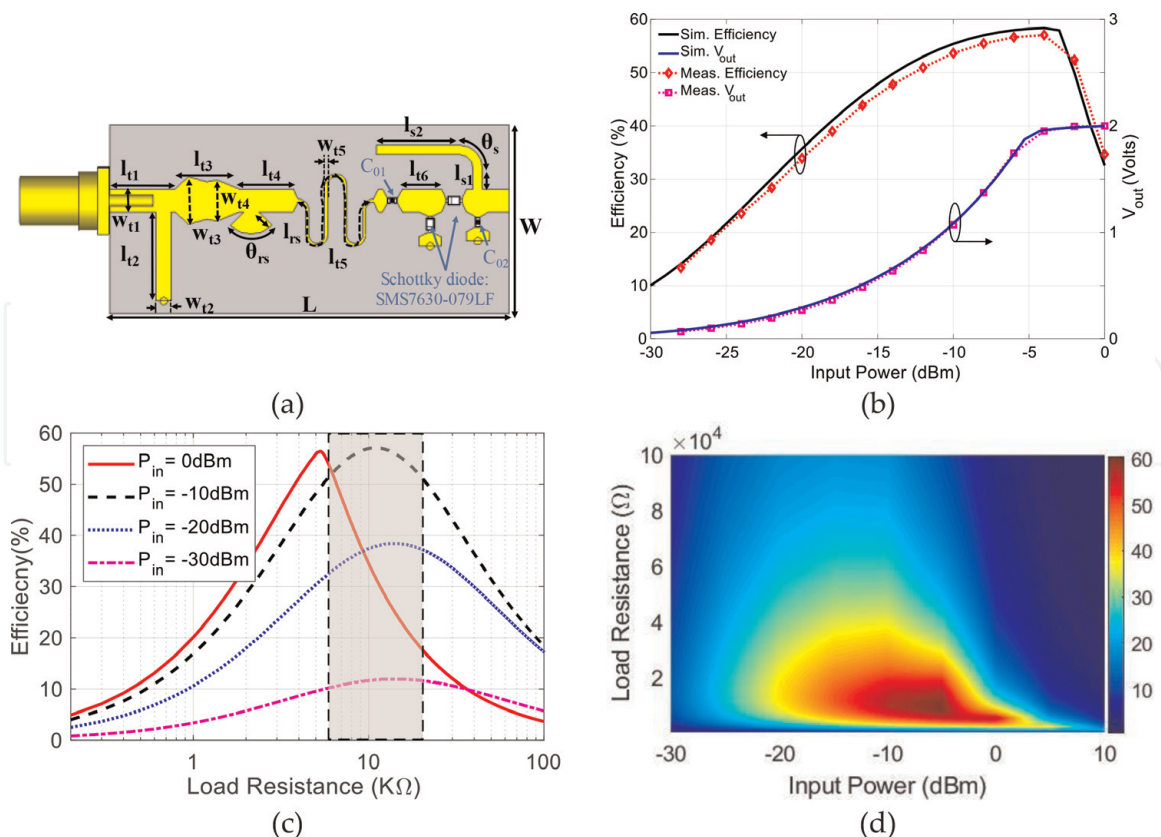


**Figure 14.** Rectifier A (a) schematic with design details, (b) simulated and measured efficiency vs. input power, (c) efficiency versus termination load, and (d) efficiency as a function of input power and the load resistance. All dimensions are in mm:  $L = 43$ ,  $l_{t1} = 7$ ,  $l_{t2} = 9.5$ ,  $l_{t3} = 6.85$ ,  $l_{t4} = 5.67$ ,  $l_{t5} = 7$ ,  $l_{t6} = 4.14$ ,  $l_{rs} = 2$ ,  $l_{s1} = 2.2$ ,  $l_{s2} = 8.75$ ,  $W = 20$ ,  $w_{t1} = 2.4$ ,  $w_{t2} = 1.6$ ,  $w_{t3} = 5$ ,  $w_{t4} = 4.35$ ,  $w_{t5} = 0.315$ ,  $\theta_{rs} = 60^\circ$ , and  $\theta_s = 90^\circ$ .

combined effect of the input power and the termination load can be seen in the chart presented in **Figure 14c**, which presents the achieved efficiency when both input power and termination load are varied logarithmically.

### 3. Rectenna design

For most of the applications presented in the introduction, the rectifiers are not used as stand-alone components but they are part of a rectenna or a multi-stage energy harvesting system. In the literature, the term rectenna refers to the combination of an antenna cascaded with a rectifier which can convert a wirelessly received RF signal into DC voltage. This section presents a voltage doubler rectenna implementation, with a directive patch antenna suitable for targeted wireless power transfer. Another rectenna implementation with an omni-directional printed inverted F antenna (PIFA) suitable for collecting ambient RF power from random directions is presented as part of the energy harvesting discussed in the subsequent Section 4.

The implemented rectangular microstrip patch antenna has 7.6 dBi gain and 97% simulated radiation efficiency radiating effectively at 5.6 GHz. Good matching is ensured using an inset-microstrip line that has characteristic impedance 50  $\Omega$ . The directive patch antenna is cascaded with a rectifier, which is first implemented as a stand-alone device on the same Duroid material. The two standalone devices with their S-parameter measurements can be seen in **Figure 15a** and **b**. For the integration of the two components, full-wave simulations using lumped ports at the common connection point were carried out in CST Microwave Studio to take into account the effect of the radiating element on the performance of the rectifier.

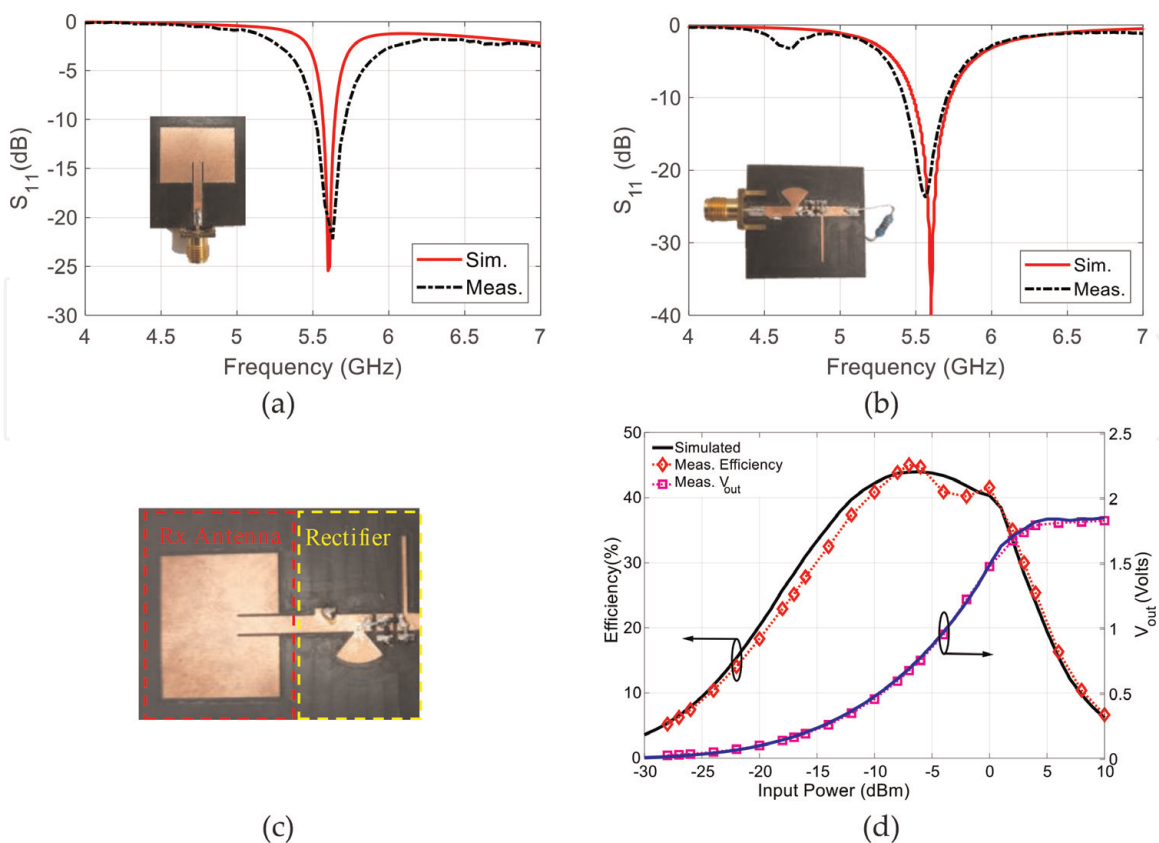


**Figure 15.** 5.6 GHz rectenna system; simulated and measured  $|S_{11}|$  (a) of rectangular patch antenna, (b) 5.6 GHz rectifier, (c) 5.6 GHz rectenna on Roger RT/Duroid5880, and (d) simulated and measured efficiency and rectified voltage vs. input power [9].

The diodes and the lumped capacitors were modeled using .s2p files in Circuit Design studio for co-simulations of the integrated module.

The integrated single-board directive rectenna can be seen in **Figure 15c**, and it can be used for far field wireless charging when the direction of arrival (DoA) is known and the directivity of the rectenna is aligned with it. The maximum implemented efficiency is around 43% and it occurs for  $-7$  dBm input power.

#### 4. Energy harvesting circuit

When energy harvesting (EH) or wireless power transfer (WPT) is used, the rectified DC voltage can be either temporarily stored until it reaches certain level, or it can be used directly without the need of any storage device. The most common storage devices are either rechargeable batteries or capacitors. When the rectified DC voltage is not stored, usually some kind of booster is needed in order to increase the low DC voltage level to make it suitable for the device that needs to be powered. Furthermore, the addition of subsequent stages unavoidably decreases the overall RF-to-DC efficiency. However, in many cases, the use of a booster is necessary. Boosters can be either active which means that an external DC power source is used to bias the booster, or it can be entirely passive. The schematic of such an EH system is presented in **Figure 16**. In this section, the implementation of an energy harvesting circuit that consists of an omnidirectional PIFA antenna and a voltage doubler matched at 1.6 GHz, cascaded with an active DC-to-DC boost converter is discussed.

The module, which is presented in **Figure 17**, was built on a Rogers 4003 material as a system on package (SoP) using a milling machine for the traces and the landing pads. The required lumped components, inductors, capacitors, Schottky diodes, and the IC module were manually soldered on the traces. The PIFA used is presented in the inset photograph of **Figure 17a** along with the measured  $|S_{11}|$ , and the implemented voltage doubler presented in the inset photograph of **Figure 17b** along with its  $|S_{11}|$ . Considering the space limitations, the rectifier was designed in a  $\Gamma$ -shape, and radial stubs were used to ensure wideband matching in order to overcome the  $|S_{11}|$  resonance shift in correspondence to the input power variations. The rectifier was terminated with the DC-to-DC booster built around the Texas Instruments TPS60301 charge pump IC model [21] that can be seen in **Figure 18a**. As mentioned earlier, the RF-to-DC efficiency depends on the termination load which in this case it is equal to the input impedance of the subsequent booster device. Although the input impedance of the power booster depends on its operation conditions, it is approximated to be  $5.1 \text{ K}\Omega$ , and this is the assumed termination load for the rectifier design.

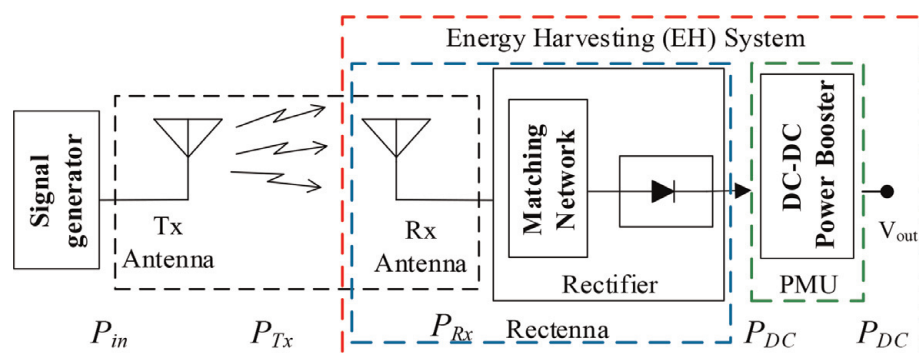


**Figure 16.**  
 Schematic diagram of RF energy harvesting system.



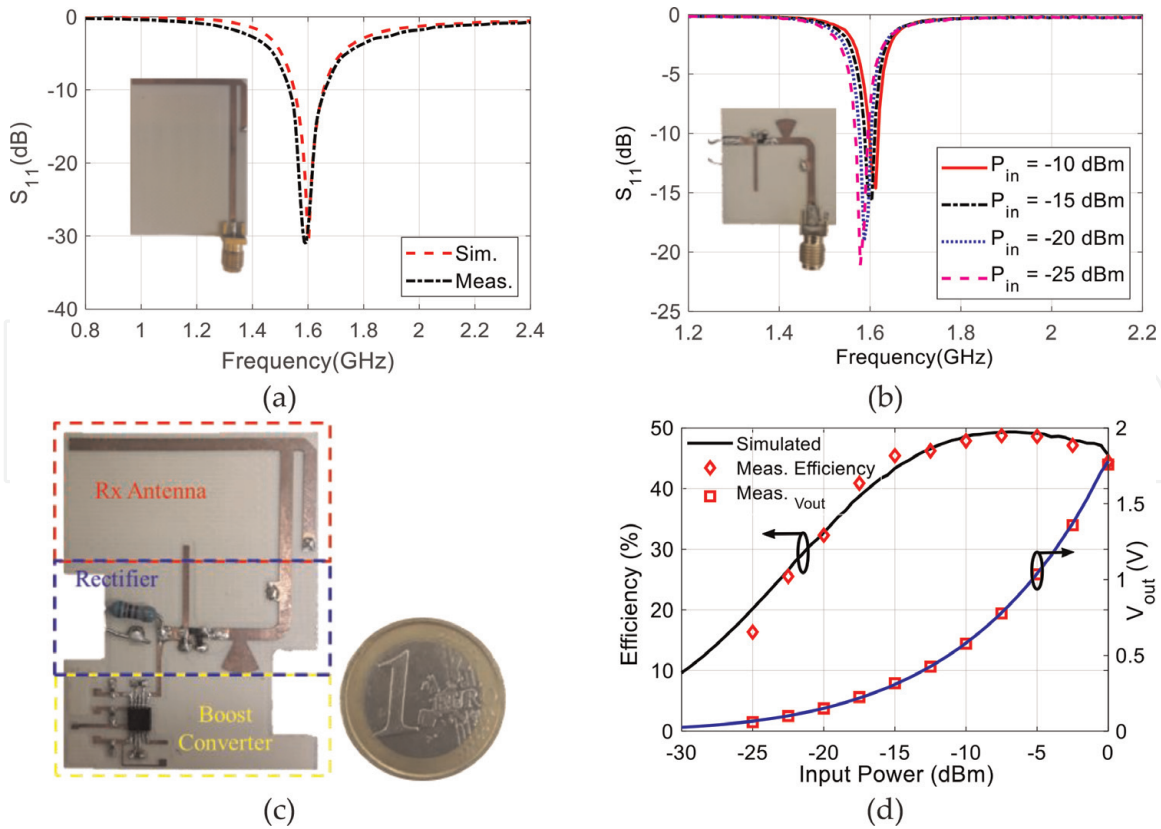


**Figure 17.** 1.6 GHz energy harvesting system (a) simulated and measured  $|S_{11}|$  of PIFA antennae, (b) measured  $|S_{11}|$  of 1.6 GHz rectifier, (c) 1.6 GHz rectenna system on Roger RO4003C, and (d) simulated and measured efficiency and rectified voltage vs. input power [10].

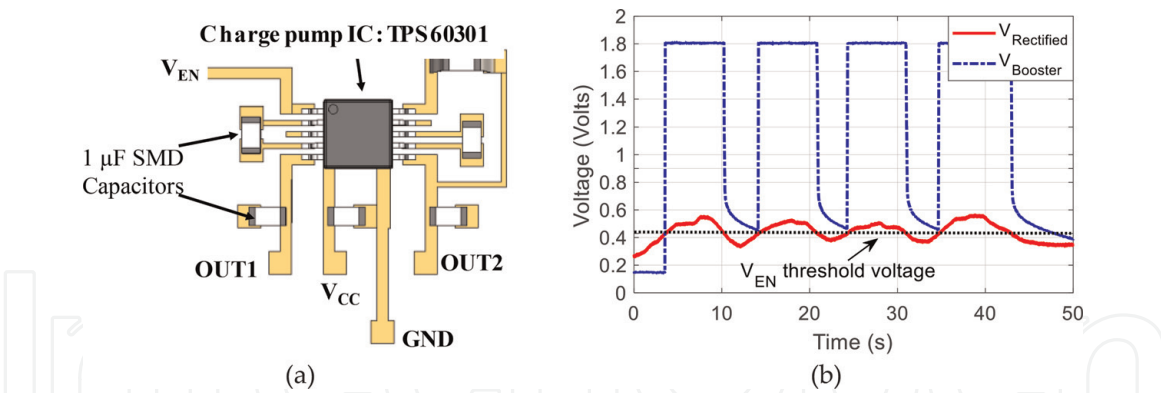


**Figure 18.** Power management unit (a) schematic of DC-to-DC power booster and (b) measured voltage across DC-to-DC power booster and rectifier output with variable distance between transmitter and rectenna at 15 dBm transmitted power from the signal generator [10].

As can be seen in the IC schematic, the enabling terminal (EN) must be connected with the output of the voltage doubler. When the rectified voltage and thus the  $V_{EN}$  voltage gets higher than 0.43 V, the DC voltage on the output terminal becomes equal to the  $V_{CC}$  biasing voltage, which can be anywhere between 0.9 and 1.8 V. This way the DC-to-DC booster output voltage can be elevated up to 1.8 V assuming that the rectified voltage is higher than 0.43 V. **Figure 18b** indicates how the output voltage of the booster ( $V_{Booster}$ ) goes from 0 to 1.8 V depending on the continuous variation of the rectified voltage at the output of the voltage-doubler rectifier ( $V_{Rectified}$ ) and whether this is larger or smaller than the minimum  $V_{EN}$  voltage, which is 0.43 V.

## 5. Conclusion

For many WPT applications, the voltage doubler is the preferred rectifier topology. This book chapter has outlined the operating principles of voltage-doubler rectifiers and has presented the most important design considerations for the implementation of such rectifying devices as standalone circuits. It has also presented examples of the use of voltage-doubler rectifiers as part of a directive rectenna system and as part of an energy harvesting system where a voltage-doubler rectifier was cascaded with an active DC-to-DC booster, demonstrating the successful implementation of wireless power transfer systems using voltage-doubler circuits as the preferred rectifier topologies.

## Acknowledgements

This research was partially funded from the Cyprus RPF, under the RESTART 2016-2020 projects: SWITCH-EXCELLENCE/1216/376 and RF-META-INFRASTRUCTURES/1216/0042. The authors would like to thank Dr. Muhammad Babar Ali Abbasi from the Centre of Wireless Innovation (CWI) at Queen's University Belfast UK for his assistance and contribution.

## Conflict of interest

All authors listed have contributed sufficiently to the project to be included as authors. The authors declare that there is no conflict of interest, financial or other regarding the publication of this book chapter.

## Author details


Abdul Quddious<sup>1\*</sup>, Marco A. Antoniadou<sup>1</sup>, Photos Vryonides<sup>2</sup>  
and Symeon Nikolaou<sup>2</sup>

<sup>1</sup> Department of Electrical and Computer Engineering, University of Cyprus, Nicosia, Cyprus

<sup>2</sup> Frederick University and Frederick Research Center, Nicosia, Cyprus

\*Address all correspondence to: [quddious.abdul@ucy.ac.cy](mailto:quddious.abdul@ucy.ac.cy)

## IntechOpen

© 2019 The Author(s). Licensee IntechOpen. This chapter is distributed under the terms of the Creative Commons Attribution License (<http://creativecommons.org/licenses/by/3.0/>), which permits unrestricted use, distribution, and reproduction in any medium, provided the original work is properly cited. 

## References

- [1] Zhang H, Guo YX, Zhong Z, Wu W. Cooperative integration of RF energy harvesting and dedicated WPT for wireless sensor networks. *IEEE Microwave and Wireless Components Letters*. 2019;**29**(4):291-293. DOI: 10.1109/LMWC.2019.2902047
- [2] Kim S, Vyas R, Bito J, Niotaki K, Collado A, Georgiadis A, et al. Ambient RF energy-harvesting technologies for self-sustainable standalone wireless sensor platforms. *Proceedings of the IEEE*. 2014;**102**(11): 1649-1666. DOI: 10.1109/JPROC.2014.2357031
- [3] Vandelle E, Vuong TP, Ardila G, Wu K, Hemour S. Harvesting ambient RF energy efficiently with optimal angular coverage. *IEEE Transactions on Antennas and Propagation*. 2018;**67**(3): 1862-1873. DOI: 10.1109/TAP.2018.2888957
- [4] Valenta CR, Durgin GD. Harvesting wireless power: Survey of energy-harvester conversion efficiency in far-field, wireless power transfer systems. *IEEE Microwave Magazine*. 2014;**15**(4): 108-120. DOI: 10.1109/MMM.2014.2309499
- [5] Mansour MM, Kanaya H. High-efficient broadband CPW RF rectifier for wireless energy harvesting. *IEEE Microwave and Wireless Components Letters*. 2019;**29**(4):288-290. DOI: 10.1109/LMWC.2019.2902461
- [6] Zhang Q, Ou JH, Wu Z, Tan HZ. Novel microwave rectifier optimizing method and its application in rectenna designs. *IEEE Access*. 2018;**6**: 53557-53565. DOI: 10.1109/ACCESS.2018.2871087
- [7] Neophytou K, Antoniadis MA. DC voltage boosting technique in RF wireless power transfer systems utilizing high PAPR digital modulations. *IET Microwaves, Antennas and Propagation*. 2019. DOI: 10.1049/iet-map.2018.5888
- [8] Pan N, Belo D, Rajabi M, Schreurs D, Carvalho NB, Pollin S. Bandwidth analysis of RF-DC converters under multisine excitation. *IEEE Transactions on Microwave Theory and Techniques*. 2017;**66**(2):791-802. DOI: 10.1109/TMTT.2017.2757473
- [9] Quddious A, Abbasi MA, Tahir FA, Antoniadis MA, Vryonides P, Nikolaou S. UWB antenna with dynamically reconfigurable notch-band using rectenna and active booster. *IET Microwave Antennas and Propagation*. 2019. DOI: 10.1049/iet-map.2018.56642019
- [10] Quddious A, Abbasi MA, Saghir A, Arain S, Antoniadis MA, Polycarpou A, et al. Dynamically reconfigurable SIR filter using rectenna and active booster. *IEEE Transactions on Microwave Theory and Techniques*. 2019;**67**(4):1504-1515. DOI: 10.1109/TMTT.2019.2891524
- [11] Quddious A, Abbasi MA, Vryonides P, Nikolaou S, Antoniadis MA, Manhaval B, et al. Reconfigurable notch-band UWB antenna with RF-to-DC rectifier for dynamic reconfigurability. In: 2018 IEEE International Symposium on Antennas and Propagation and USNC/URSI National Radio Science Meeting. IEEE; 8th July; 2018. pp. 283-284. DOI: 10.1109/APUSNCURSINRSM.2018.8608685
- [12] Quddious A, Abbasi MA, Tariq MH, Antoniadis MA, Vryonides P, Nikolaou S. On the use of tunable power splitter for simultaneous wireless information and power transfer receivers. *International Journal of*

Antennas and Propagation. 2018;**2018**:  
12. DOI: 10.1155/2018/6183412. Article  
no: 6183412

[13] Pournoori N, Khan MW, Ukkonen L, Björninen T. RF energy harvesting system integrating a passive UHF RFID tag as a charge storage indicator. In: 2018 IEEE International Symposium on Antennas and Propagation and USNC/URSI National Radio Science Meeting. IEEE; 8th July; 2018. pp. 685-686. DOI: 10.1109/APUSNCURSINRSM.2018.8608530

[14] Tentzeris MM, Nikolaou S. RFID-enabled ultrasensitive wireless sensors utilizing inkjet-printed antennas and carbon nanotubes for gas detection applications. In: 2009 IEEE International Conference on Microwaves, Communications, Antennas and Electronics Systems. IEEE; 9th November; 2009. pp. 1-5. DOI: 10.1109/COMCAS.2009.5385940

[15] Rida A, Yang L, Reynolds T, Tan E, Nikolaou S, Tentzeris MM. Inkjet-printing UHF antenna for RFID and sensing applications on liquid crystal polymer. In: 2009 IEEE Antennas and Propagation Society International Symposium. IEEE; 1st June; 2009. pp. 1-4. DOI: 10.1109/APS.2009.5171791

[16] Rida A, Nikolaou S, Tentzeris MM. Broadband UHF RFID/sensor modules for pervasive cognition applications. In: 2009 3rd European Conference on Antennas and Propagation. IEEE; 23rd March 2009. pp. 2344-2347

[17] Abdulhadi AE, Abhari R. Multiport UHF RFID-tag antenna for enhanced energy harvesting of self-powered wireless sensors. IEEE Transactions on Industrial Informatics. 2015;**12**(2): 801-808. DOI: 10.1109/TII.2015.2470538

[18] Yuan F. CMOS Circuits for Passive Wireless Microsystems. New York:

Springer; 2011. DOI: 10.1007/978-1-4419-7680-2

[19] Skyworks. Solutions. (February). Schottky Diode [online]. Available from: <http://www.skyworksinc.com/Product/511/SMS7630> [Accessed: February, 2019]

[20] Broadcom Inc. (February). Schottky Diode [online]. Available from: [https://docs.broadcom.com/docs/hsms-285x\\_equivalent\\_circuit](https://docs.broadcom.com/docs/hsms-285x_equivalent_circuit) [Accessed: February, 2019]

[21] Texas Instruments (February). Charge Pump IC: TPS60301. Available from: <http://www.ti.com/product/TPS60301> [Accessed: February, 2019]